Hindawi
Mathematical Problems in Engineering
Volume 2020, Article ID 3731749, 20 pages
https://doi.org/10.1155/2020/3731749

Research Article

NSGA-II-Based Parameter Tuning Method and GM(1,1)-Based Development of Fuzzy Immune PID Controller for Automatic Train Operation System

Pengzi Chu,[1,2,3] **Yi Yu**,[2,3] **Danyang Dong**,[2,4] **Hui Lin**,[2,3] **and Jianjun Yuan**[2,3,4]

[1]*The Key Laboratory of Road and Traffic Engineering, Ministry of Education, Tongji University, Shanghai 201804, China*
[2]*Tongji University Maglev Transportation Engineering R&D Centre, Tongji University, Shanghai 201804, China*
[3]*Shanghai Maglev and Rail Transit Collaborative Innovation Centre, Tongji University, Shanghai 201804, China*
[4]*College of Electronics and Information Engineering, Tongji University, Shanghai 201804, China*

Correspondence should be addressed to Yi Yu; yuyi1962@tongji.edu.cn and Jianjun Yuan; yuanjianjun@tongji.edu.cn

Received 29 November 2019; Revised 18 February 2020; Accepted 25 February 2020; Published 24 March 2020

Academic Editor: Alessandro Gasparetto

Automatic train operation (ATO) system is one of the important components in advanced train operation control systems. Ideal controllers are expected for the automatic driving function of ATO systems. Aiming at the intelligence requirements of the systems, an NSGA-II-based parameter tuning method for the fuzzy immune PID (FI-PID) controller and a grey model GM(1,1)-based fuzzy grey immune PID (FGI-PID) controller were proposed. Taking a maglev train's model as the control object and a velocity-time curve as the input, the feasibility of the parameter tuning method for the FI-PID controller and the applicability of the FI-PID controller and the FGI-PID controller for the ATO system were tested. The results showed that the optimized parameters were ideal, the two controllers all showed good performance on the indicators of traceability and comfort level, and the FGI-PID controller performed better than the FI-PID controller. The results exhibited the effectiveness of the proposed methods.

1. Introduction

Railways have the advantages of large volume, speed, safety, and low pollution. Many countries in the world have complex railway networks, and many cities also have developed subway networks, which greatly facilitate a person's travel. The railway technology worldwide tends to develop in the directions of seriation, specialization, and diversification. The types of the trains are also diverse, such as wheel/rail trains, maglev trains, and trams. Advanced passenger trains have automatic driving capabilities that can improve operation efficiency and reduce driver's workload, and the automatic train operation (ATO) system is vital to achieve these functions. For improving comfort and stopping accuracy, and energy saving, a driverless train needs a very stable ATO system.

The speed curve and the speed curve tracking ability are two keys to optimize ATO systems [1–3]. The accuracy of speed curve tracking is related to the adopted control method. The proportion-integration-differentiation (PID) controller is widely used in industrial control, due to its advantages of simple control structure, wide application, and easy to implement. In order to ensure a good control effect, repeated tuning of control parameters is a common procedure in the current field of engineering. However, most industrial processes, including the ATO systems, have dynamic characteristics. Once the control parameters are fixed, the ideal stopping accuracy and comfort cannot be completely guaranteed. Therefore, the tuning and self-tuning of the PID controller or other controllers have attracted much attention.

With the rapid advancement to fully automatic operation (FAO) mode of railways, the key role of ATO systems [4, 5] has become more and more prominent in the control layer. Practically, safety, comfort, and energy saving are significant problems concerned by railway operators and manufacturers. The purpose of this study is to find an effective controller for an ATO system, including its tuning and development.

1.1. Literature Review. A large number of industrial processes belong to the control processes, and the proper control parameters are the guarantee for a good control effect. The Ziegler–Nichols (Z-N) method and the Tyreus–Luyben (T-L) method are classical methods for the tuning of the PID controller. Using intelligent algorithms to tune control parameters offline is also an efficient way. Xue et al. [6] used particle swarm optimization (PSO), Z-N method, and advanced fireworks (AFW) algorithm to tune a PID controller and found that AFW algorithm was more effective than the others. Mahdavian et al. [7] used nondominated sorting genetic algorithm-II (NSGA-II) to optimize the control parameters of a PID controller and found that NSGA-II had more advantages than Z-N method. Behroozsarand and Shafiei [8] also designed NSGA-II to tune a PID controller and obtained better control parameters than the T–L method. Chen et al. [9] used chaotic NSGA-II to tune the five parameters of the fractional-order PID controller. Özdemir et al. [10] developed a bacterial swarm optimization (BSO) algorithm based on PSO algorithm and bacterial foraging optimization (BFO) algorithm to optimize the control parameters of the PID controller and the fractional-order PID controller. Zhao et al. [11] designed a two-lbest multiobjective PSO algorithm to tune the multiobjective robust PID controller, and the simulation result showed a relatively better performance. Reynoso-Meza et al. [12] used an algorithm based on the differential evolution technique and spherical pruning to tune the parameters of the PI controller. Rahmani et al. [13] tuned a novel supertwisting PID sliding mode controller based on the multiobjective bat algorithm. Wang et al. [14] applied a mutative scale chaos optimization method to optimize control parameters of the fuzzy immune PID (FI-PID) controller. Ma and Gu [15] designed a PSO algorithm to tune the FI-PID controller.

With the help of added parameters and introduced algorithms, adaptive controllers or self-tuning controllers have attracted many attentions because they can effectively deal with dynamic control processes. Wang and Xiao [16] implemented the PID controller's self-tuning through the pole assignment optimal prediction algorithm. Kim [17] designed a PID controller with an analyser of gain/phase margin and immune algorithm. Mendes et al. [18] discussed several self-tuning controllers (STCs) with PID form based on explicit and implicit identification algorithms. Wai and Lee [19] designed an adaptive fuzzy-neural-network control (AFNNC) scheme to overcome the highly nonlinear and unstable characteristics of a control object. Majdabadi-Farahani et al. [20] introduced a method for the PID controller self-tuning online based on model predictive control and used NSGA-II for parameter tuning of the predictive model. Wang and Bian [21] combined BP neural network and genetic algorithm (GA) to tune three parameters of the PID controller online.

The process of train operation is also a typical control process. The PID controller is used widely in current ATO systems. Many advanced controllers have been tested for the applicability in ATO systems. Oshima et al. [22] and Yasunobu et al. [23] proposed two controllers based on fuzzy theory. Gao et al. [24] proposed an adaptive fault-tolerant control algorithm by RBF neural networks. Mo et al. [25] designed an ATO automatic speed control algorithm in conjunction with a prediction algorithm and a multivariable fuzzy control algorithm. Fu et al. [26] proposed a PSO-B-BP-PID controller by combining a reparametric b-spline neural network and PSO algorithm. Wu [27] proposed a method named adaptive terminal sliding mode control. Cao et al. [1] and Liu et al. [2] designed a sliding mode controller and a predictive control algorithm, respectively, for the ATO systems to track the optimized target speed curve and found that they have superiority compared with the PID controller. Ke et al. [3] used the MAX–MIN ant system to optimize the target speed curve and designed a fuzzy PID controller to track the speed curve. Shi [28] introduced a model-free adaptive control method to track the ATO target speed curve and exhibited a good speed curve tracking effect. Hou et al. [29] designed a predictive fuzzy adaptive PID controller for a high-speed train's speed control. Long et al. [30] proposed an auto-disturbance-rejection control algorithm for a maglev ATO system.

1.2. Proposed Approaches. As an intelligent algorithm, the fuzzy algorithm is widely used in control processes [15, 19, 22, 29]. The general fuzzy control method needs a number of fuzzy conditional statements in the form "if ... then ..." with fuzzy sets, but the fuzzy immune PID (FI-PID) controller can achieve ideal control with few fuzzy conditional statements [3, 31–33]. To the best of our knowledge, the applicability of the FI-PID controller in ATO systems and its tuning based on nondominated sorting genetic algorithm-II (NSGA-II) have not been discussed. The FI-PID controller is considered to optimize ATO systems, and its tuning problem is also discussed in this study. Meanwhile, the maglev train is one of the latest trends in railways around the world, more and more studies focus on the safe operation of the promising train [19, 30, 34, 35], and a model of the maglev train's ATO system is used as a controlled object. The main contributions of this paper are summarized as follows:

(1) In order to assist the tuning of the FI-PID controller, a framework based on NSGA-II was proposed. The optimization of parameters is very important for the performance of the PID controller or the FI-PID controller [32, 36]. The problem is often multiobjective, and NSGA-II can solve almost any multiobjective optimization problem [7]. Multiple optimal solution sets of control parameters are

solved based on NSGA-II and three objective functions. The sets of optimal parameters are further processed by post Pareto-optimal to determine the final optimal solutions for decision makers. The simulation results show that the optimal parameters are helpful for good control performances.

(2) Considering the superiority of self-tuning controllers and the possibility for further optimizing the FI-PID controller, a novel FGI-PID controller integrating the FI-PID controller and a prediction algorithm is proposed. Predictive control methods can usually achieve better control effects [20, 29, 37, 38], and this study attempts to expand the FI-PID controller with the prediction algorithm named GM(1,1) [39, 40]. In the FGI-PID controller, a grey adjuster based on the GM(1,1) is added to the FI-PID controller. The simulation results show that, compared to the FI-PID controller, the FGI-PID controller has a better performance with the same optimized parameters.

The remainder of this paper is organized as follows. Section 2 describes the general automatic train control (ATC) system, the existing train's dynamic models, and the dynamic model used in the study. In Section 3, the principle of the FI-PID controller is described, the NSGA-II based FI-PID parameter tuning framework is proposed, and 10 optimized parameter sets are obtained. In Section 4, the grey model GM(1,1) is summarized, and the principle of the FGI-PID controller is proposed. Then, in Section 5, the FI-PID controller and the FGI-PID controller with the optimized parameters are used for tracking tests with a velocity-time curve, and the performances of the FI-PID controller and the FGI-PID controller are compared from traceability and comfort. Sections 6 and 7 are discussion and conclusion of the study, respectively.

2. ATO System and Train's Dynamic Model

As a key subsystem of an operation control system, ATO system is the basis for the automatic driving, the efficient operation, and the safe operation of a train. As demonstrated in Figure 1, for general automatic train control (ATC) system of wheel/rail vehicle, onboard ATO system receives ground information and driving control commands from automatic train protection (ATP) system and automatic train supervision (ATS) system and performs a task of traction or braking automatically [41, 42].

It is worth mentioning that the operation of wheel/rail vehicles is driven by onboard rotary motors, but the traction of normal maglev vehicles comes from tracks based on linear synchronous motors. ATO systems realize automatic driving by mutual linkage with traction systems. Therefore, there are differences in the composition of maglev transportation operation control systems and wheel/rail transportation operation control systems, especially on the locations and names of ATO-related equipment. Although there are differences between the two modes of transportation, their functions are similar and can be referred to each other.

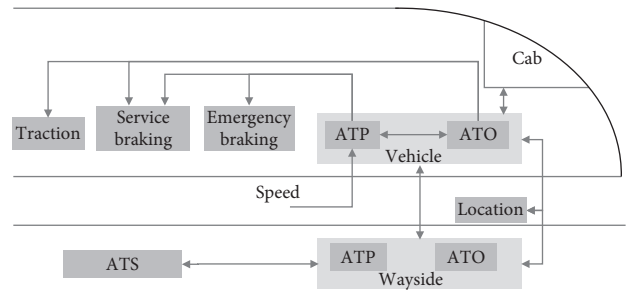

Figure 1: General ATC system.

As one kind of complex system covering a broad range of professional fields, the operation process of a train is nonlinear and uncertain, which needs a controller to keep stable. The existing train's dynamic models are also diverse, such as an equation of state model [27], a second-order transfer function [43], a first-order transfer function with transmission delay [44], and a transfer function established for a maglev train [4, 5, 30, 45–49]. In this study, the model of the maglev train was adapted as the control object, which can be expressed as

$$G(s) = \frac{612}{s + 0.34} \frac{1}{8621s + 822.4} = \frac{0.07128}{(s + 0.0954)(s + 0.34)}. \tag{1}$$

The typical frequency of control messages is about 100–600 milliseconds, and shorter than 100 milliseconds it is normally supported [42, 50]. In this study, the sampling time was set as 100 milliseconds by referring Xu and Xiao [45]. And the discretized model of Formula (1) is

$$G(z) = \frac{0.0003513z + 0.0003462}{z^2 - 1.957z + 0.9574}. \tag{2}$$

3. NSGA-II-Based Parameter Tuning Framework

In practical applications, in order to achieve an acceptable control performance, it is necessary to find a set of ideal control parameters for a certain controller. The manual parameter tuning method is difficult for this purpose, and there is currently no classical parameter tuning method for the FI-PID controller. The study discusses a tuning framework for the controller based on NSGA-II.

3.1. FI-PID Controller. When antigens invade the body, the constituent elements of the lymphocyte helper T cell T_H, the suppressor T cell T_S, and the B cell cooperate with each other for the balance of immune feedback system. Based on the adaptive mechanism of the immune process, the increment PID controller, and the fuzzy control method, the FI-PID controller was designed by taking the number of antigens as error, the total stimulus received by B cells as the control signal or control law [51, 52]. Meanwhile, the controller introduces two variables namely the rate of reaction K and the coefficient of stabilizing effect η, and set

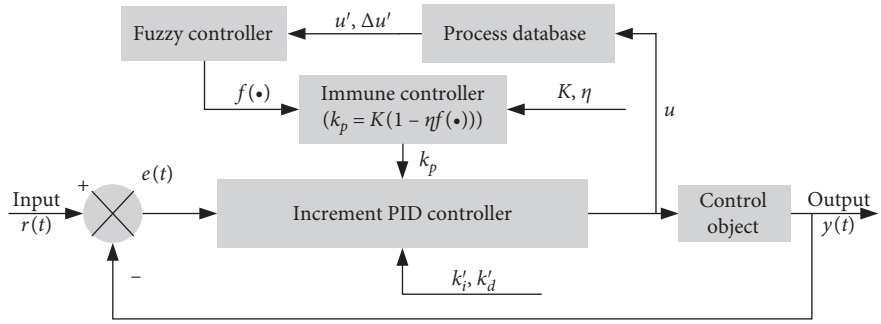

Figure 2: Structure of the FI-PID controller.

$k_p = K(1 - \eta f(u'(t), \Delta u'(t)))$. Then, the structure of the FI-PID controller is shown in Figure 2.

The control law $u(t)$ of the controller is

$$u(t) = u(t-1) + k_p\left((e(t) - e(t-1)) + k_i' e(t) + k_d'(e(t) - 2e(t-1) + e(t-2))\right), \tag{3}$$

where $f(\cdot)$ is the fuzzy logic function, k_i' is the integral coefficient, k_d' is the differential coefficient, $u'(t)$ and $\Delta u'(t)$ are the simplified expressions of $u(t-1)$ and $u(t-1) - u(t-2)$, respectively, and $e(t)$ is the deviation between input and output, which equals $r(t) - y(t)$, as shown in Figure 2. The pseudocode corresponding to the simulation process of FI-PID is shown as follows (Algorithm 1).

For the fuzzy rules of the controller in this study, each input variable was blurred into "positive" (P) and "negative" (N), respectively. And output variables were blurred to "positive" (P), "zero" (Z), and "negative" (N), and the membership function was defined in the entire interval of $(-\infty, +\infty)$. The fuzzy rule adopted for $f(\cdot)$ was as follows: if u is positive and Δu is positive, then $f(\cdot)$ is negative; if u is positive and Δu is negative, then $f(\cdot)$ is zero; if u is negative and Δu is positive, then $f(\cdot)$ is zero; if u is negative and Δu is negative, then $f(\cdot)$ is positive. For the rules, Zadeh fuzzy logic "AND" and the usual "mom" defuzzifier were employed to acquire an output of the fuzzy controller $f(\cdot)$ [14, 52]. Based on the settings above, the fuzzy controller of the FI-PID controller contains two inputs, one output and four fuzzy rules, as shown in Figure 3.

3.2. Parameters Tuning Method. For FI-PID controllers, there are four parameters that need to be tuned, including the rate of reaction K, the coefficient of stabilizing effect η, the integral coefficient k_i', and the differential coefficient k_d' [14, 15]. Appropriate optimization objectives are important for parameter tuning, and it is a multiobjective optimization problem in general [7–11]. With an optimization model and a corresponding algorithm, an optimization process was introduced to solve this problem in the study.

3.2.1. Objective Functions and Solution. For ATO system or other similar systems, the purpose of parameter tuning is to reduce the deviation between input and output. Errors were widely discussed in parameter optimization [9, 10, 51, 53, 54]. Taking error as the basic point, a multiobjective optimization model was put forward from the three aspects of train's operation, including overall operation, initial acceleration phase, braking, and stopping phase. And the optimization model and its subobjective functions are

$$\text{Min } F = \{f_1, f_2, f_3\}, \tag{4}$$

$$f_1 = \int_0^m |e(t)|\mathrm{d}t, \tag{5}$$

$$f_2 = \int_0^m \left(t^{-1}\right) e^2(t)\mathrm{d}t, \tag{6}$$

$$f_3 = \int_0^m t e^2(t)\mathrm{d}t, \tag{7}$$

where the first optimization object is integrated absolute error (IAE) [10, 53], which considers the overall error equally; the second optimization object is integral of time's reciprocal multiplied by squared error (ITRSE), which focuses on the error in the initial stage, and less considers the error in the later stage; the third optimization object is the integral of time multiplied by squared error (ITSE) [9, 10], which less considers the error in the initial stage, but focuses on errors in later stage; m is the length of an error sequence, $e(t)$ is the tth error in error sequence, and m and t are all integers in the study.

Seeking a set of nondominated optimal solutions or Pareto solutions is the goal of a multiobjective optimization problem [55]. For two solutions p and q, if the condition "for $i = 1, 2, 3$, and objective functions $f_i(p) < f_i(q)$" is met, then p dominates q, and p is the nondominated solution. If the condition "for $i = 1, 2, 3$, objective functions $f_i(p) \le f_i(q)$, and at least one j belonging to $1, 2, 3$ satisfy $f_j(p) < f_j(q)$" is met, then p weakly dominates q, and p is also the nondominated solution. A set of nondominated solutions is the optimal solutions, namely, Pareto solutions.

Initialize the parameters (K, η, k_i', k_d', *fuzzy rules* $f(\cdot)$, control law u, initial output y, and initial error e).
while ($t \leq length\ of\ inputs$) **do**
  Calculate the current output $y(k)$ according to (1) or (2)
  Calculate current error $e(t)$
  $k_p(t) = K(1 - \eta f(u'(t), \Delta u'(t)))$
  Calculate the current control law $u(t)$ according to (3)
  Update data u, e, y
end while
Postprocess results and visualization

Algorithm 1

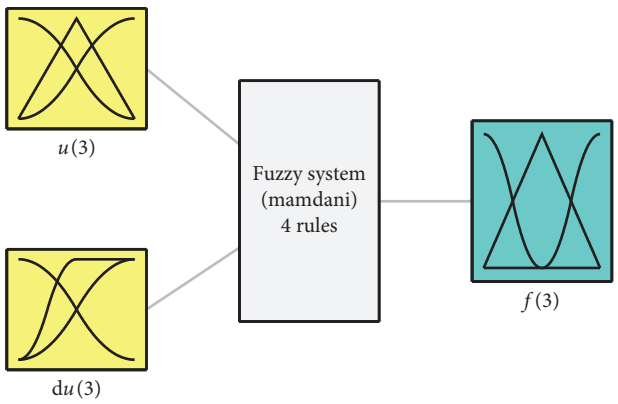

Figure 3: Structure of the fuzzy controller.

3.2.2. Optimization Algorithm and Its Process. Genetic algorithms (GA) have become a widely used method of parameter tuning in many controllers [7, 8, 21, 51, 54]. NSGA-II is a multiobjective optimization method derived from GA with an elite preservation strategy and a fast-nondominated sorting method [7, 55, 56]. NSGA-II can find optimal solutions based on initial feasible solutions. First, the algorithm randomly generates a number of individuals, which is the initial population. The fast-nondominated sorting is performed for different individuals according to their objective function fitness values. Individuals in the population are further selected based on tournament method to generate offspring based on crossover or mutation according to the preset probabilities. And the offspring are merged into the current population. Then, a new population is formed according to each individual's nondomination rank and crowding distance. By repeating the above operation continuously, the population is gradually evolved toward a set of better solutions until the preset termination condition is met. The corresponding pseudocode is shown as follows (Algorithm 2).

For individuals in GA or NSGA-II, the coding form of chromosomes needs to be designed. As mentioned above, the parameters requiring further tuning include K, η, k_i', and k_d'. To simplify the process of decoding, the study adopted decimal coding method for above parameters. Considering the storage of the objective function fitness values, nondomination rank, and crowding distance, the coding form of chromosomes was set in Figure 4.

The process of parameter tuning is shown in Figure 5, which takes a test signal and the 1st to 4th digits in an individual's code as the input of the FI-PID controller and takes the transfer function (Formula (2)) as the control object. After executing the control simulation process, the corresponding error sequence can be used to calculate the three objective function fitness values according to equations (5)–(7), and these values are stored in the 5th to 7th positions of the corresponding codes. After obtaining all fitness values of a population, the nondomination sorting and the calculation of crowding distance can be performed. The values of nondomination rank and crowding distance are stored in the 8th and 9th positions of corresponding codes.

Based on the current individuals' nondomination ranks and crowding distances, a mating pool can be formed based on the current population and the tournament method. For the tournament method, an individual with a high nondomination rank or the same nondomination rank but a large crowding distance is the winner of two individuals. The operation of crossover or mutation is performed based on these individuals in the mating pool to generate offspring, and objective function fitness values of the offspring are calculated simultaneously. Furthermore, offspring are merged with the current population, and the population that contains offspring needs to be screened to form a new population according to the nondominated ranks and crowding distances, with eliminating the bad individuals and retaining elite individuals. In the study, for generating a set of offspring, crossover operation is the exchange in 1st to 4th elements between two chromosomes according to a preset probability, and mutation operation is a random mutation of one in 1st to 4th elements of a chromosome. The above process is continuously executed until the number of iterations or other stop criterions are met, such as the quality or quantity of an optimal solution.

The final output of NSGA-II is Pareto solutions, which is one set of control parameters. However, the results of NSGA-II or other genetic algorithms are somewhat random. Although individuals in Pareto solutions do not dominate each other, there are still individuals that may not match one's expectations. For example, one fitness value in objective functions can be very unsatisfactory with other values that are ideal for an individual. Meanwhile, Pareto solutions may also contain local optimal solutions, which happened a lot in practice. Aiming at these two problems, in order to

Initialize the parameters (population size N, iterations G, crossover and mutation probabilities, mating pool size P)
Initialize N individuals randomly
for $(i = 1, 2, \ldots N)$ **do**
  Perform a simulation process of FI-PID for an individual, and update the fitness of the individual using (5)–(7)
end for
Calculate the nondominated rank and crowding distance based on the fitness value of the initial population
while $(g \leq G)$ **do**
  P individuals are selected from the current N individuals according to the tournament method
  Perform crossover or mutation on this P individuals based on according probabilities to generate offspring
  Execute the simulation process of FI-PID to obtain the fitness value of each new offspring
  Combine the offspring with the N individuals as a temporary population
  Perform the nondominated sorting and calculate crowding distances on the temporary population
  Reserve N elite individuals as new population according to nondominated ranks and crowded distances
end while
Yield a set of the optimal solutions
Postprocess results and visualization

Algorithm 2

1	2	3	4	5	6	7	8	9
K	η	k_i'	k_d'	f_1	f_2	f_3	Non-domination rank	Crowding distance

Figure 4: Coding form.

obtain better parameters, a viable approach is obtaining nondominated solutions as many as possible by performing the optimization process multiple times and further screening them with nondomination sorting and a certain criterion, as shown in Figure 6. In terms of further screening for deficient individuals in a new set of Pareto solutions, the study suggests removing individuals with extreme values.

3.3. Results of Parameters Tuning. In the study, with reference to the setting of Babaveisi et al. [57], the crossover and mutation probabilities of NSGA-II were, respectively, set as 0.8 and 0.25, and the iteration, the population size, and the mating pool size were set as 80, 25, and 19, respectively. In terms of the range of parameters, the range of K was set as $[1, 200]$, the range of η was $[0, 1]$, and k_i' was $[0, 3]$, k_d' was $[0, 30]$. Referring to the research of Utomo and Widianto [5], the study sets the input signal as a square wave with an interval of 0.1, a swing size of $[0, 1]$, a duty ratio of 0.5, and a length of 1000. The train's dynamic model (Formula (2)) was taken as the control object.

One Pareto situation was obtained according to Figure 5 without a further screening, as shown in Figure 7 and Table 1. The process took 948.128 s, which relied on the MATLAB software and a Thinkpad laptop with Version P52, CPU i7-8750H, and memory 16 GB.

Figure 7 contains 6 Pareto solutions, and Table 1 lists all the optimal solutions obtained and their objective function fitness values. The results show that the minimum value of the objective function 1 is 33.840, the minimum value of the objective function 2 is 2.037, and the minimum value of the objective function 3 is 7159.192. Since the length of the input signal is 1000, all the minimum values are ideal.

As mentioned above, genetic algorithms have randomness, and local optimal solutions are also prone to occur easily. The number of optimal solutions in Table 1 is small, and they may contain some local optimal solutions or some poor optimal solutions. In terms of this issue, the study optimized the parameters 10 times with the same method according to Figure 5 without a further screening, and 10 sets of Pareto solutions containing 148 individuals had been obtained. For these 10 sets, repetitive individuals were removed firstly, and a new set of Pareto solutions was obtained by nondominated sorting according to Figure 6. The distribution of these solutions' fitness values was shown in Figure 8.

It can be seen from Figure 8 that major individuals are dominated by a few individuals (Table 2), and these individuals are closer to the ideal point (0, 0, 0). However, there is only one solution in Table 1 located in Table 2, which shows the necessity for further optimization for one set of solutions. At the same time, considering the possible bad individuals in the optimized individuals, the individuals with a maximum fitness value had been removed from the study to further screen ideal individuals. The maximum value of objective function 1 in Table 2 is 82.011, the corresponding individual is 11, the maximum value of objective function 2 is 2.055, the corresponding individual is 6, the maximum value of objective function 3 is 9718.481, and the corresponding individual is 11. Based on the screening suggestion above, individuals 6 and 11 are deficient individuals. As shown in Figure 8, the distance of individual 11 from other optimal solutions is large. Although the individual 6 is closer

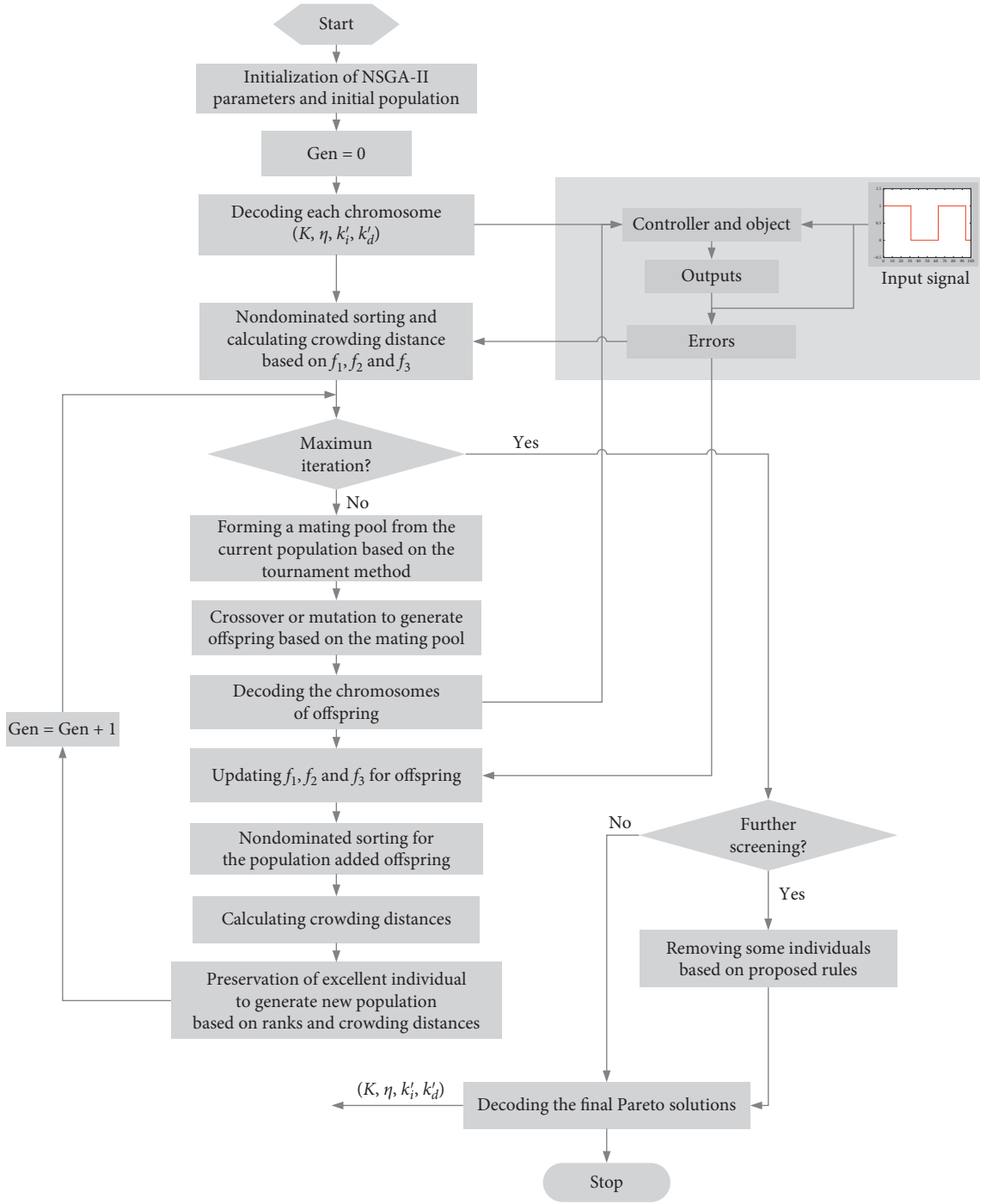

Figure 5: NSGA-II based parameters tuning framework for the FI-PID controller.

to other optimal individuals, since it contains a maximum value, it also needs to be removed according to the screening criterion in the study.

Based on the above steps, 10 optimal individuals had been obtained in the study. Each of them performed very well on the objective functions and can be tested for ATO systems.

4. FGI-PID Controller

As mentioned above, the optimal results of the genetic algorithm are stochastic,and it is difficult to obtain a set of best parameters. At the same time, it is very likely uncertain in the actual operation process of a train. For the existing optimization space, the study references the idea of predictive

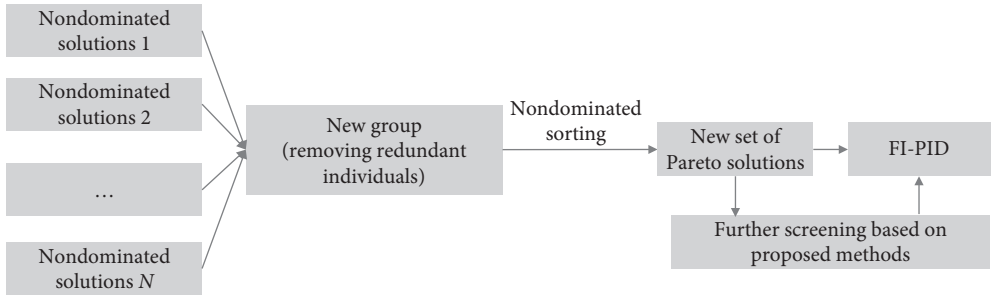

Figure 6: Screening processing for multi-Pareto solutions.

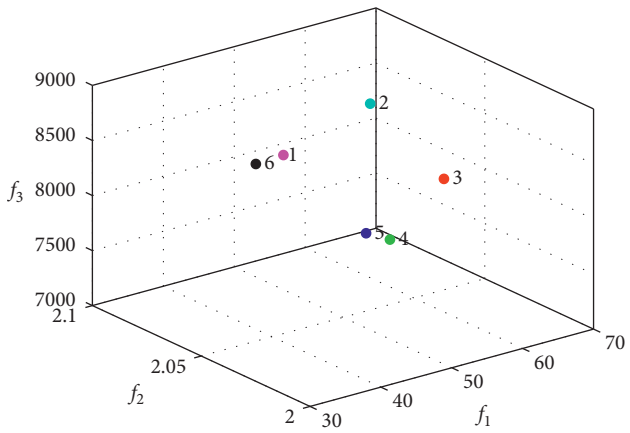

Figure 7: Distribution of a Pareto solution set.

control and further fine-tunes these tuned parameters according to current error and prediction error to explore the possibility of further optimization for the FI-PID controller.

4.1. Grey Model GM(1,1). Grey model GM(1,1) is one important part of prediction methods in grey theory. It is a first-order differential equation model with a single variable prediction, and its discrete-time response function approximates an exponential pattern [39, 40, 58]. Combined with the research content of the study, the process of GM(1,1) was summarized as follows.

Assume $e^{(0)} = \{e^{(0)}(1), e^{(0)}(2), \cdots, e^{(0)}(n)\}$ was the original sequence consisting of the sequence of error or deviation $e(t)$ between input and output. Then $e^{(1)}$ is the first-order accumulated sequence, that is, $e^{(1)} = \{e^{(1)}(1), e^{(1)}(2), \cdots, e^{(1)}(n)\}$, where $e^{(1)}(t) = \sum_{i=1}^{t} e^{(0)}(i)$, $t = 1, 2, \cdots, n$.

The Albinism differential equation of GM(1,1) is

$$\frac{de^{(1)}}{dt} + ae^{(1)} = b, \tag{8}$$

where a and b are parameter and endogenous variable to be identified.

Constructing unrecognized parameters into a vector $\widehat{a} = (a, b)^T$ obtained by least-squares method, $\widehat{a} = (B^T B)^{-1} B^T Y$, where

$$B = \begin{bmatrix} -\frac{1}{2}\left(e^{(1)}(2) + e^{(1)}(1)\right) & -\frac{1}{2}\left(e^{(1)}(3) + e^{(1)}(2)\right) & \cdots & -\frac{1}{2}\left(e^{(1)}(n) + e^{(1)}(n-1)\right) \\ 1 & 1 & \cdots & 1 \end{bmatrix}^T, \tag{9}$$

$$Y = \left[\, e^{(0)}(2) \;\; e^{(0)}(3) \;\; \cdots \;\; e^{(0)}(n) \,\right]^T. \tag{10}$$

The discrete-time response function of the prediction model is

$$e^{(1)}(t+1) = \left(e^{(0)}(1) - \frac{b}{a}\right)e^{-at} + \frac{b}{a}, \tag{11}$$

where the e of e^{-at} is the Napierian base, and $e^{(1)}(t+1)$ is the predicted value obtained by accumulating.

Then a predicted error can be restored by $\widehat{e}^{(0)}(t+1) = \widehat{e}^{(1)}(t+1) - \widehat{e}^{(1)}(t)$, where $t = 1, 2, \cdots n$. For formal simplification, a prediction error $e'(t+1) = \widehat{e}^{(0)}(t+1)$ in the study.

4.2. Design of FGI-PID Controller. The development of the FI-PID controller focuses on the immune parameters of K and η. The prediction algorithm of GM(1,1) was used to adjust these two parameters dynamically based on current errors and corresponding prediction errors. And a kind of fuzzy grey immune PID (FGI-PID) controller was raised. The structure of the FGI-PID controller was shown in Figure 9.

Different from the structure of the FI-PID controller (Figure 2), there is an adjusted part for the immune controller to adjust the parameters of K and η. As shown in

Table 1: Parameters and fitness in a set of Pareto solutions.

No.	K	η	k_i'	k_d'	f_1	f_2	f_3
1	117.483 072	0.004 112	4.535 228	20.815 663	45.478 970	2.062 627	8437.193 409
2	117.483 072	0.365 846	5.189 957	20.815 663	63.098 630	2.080 257	8434.407 945
3	127.711 245	0.004 112	4.535 228	20.815 663	66.323 764	2.056 862	7908.307 087
4	127.711 245	0.004 112	5.189 957	20.815 663	65.360 173	2.078 545	7175.785 564
5	127.711 245	0.004 112	5.648 306	20.815 663	64.781 421	2.087 611	7159.192 661
6	196.056 906	0.0041 12	2.483 254	11.076 463	33.840 311	2.037 480	8790.987 535

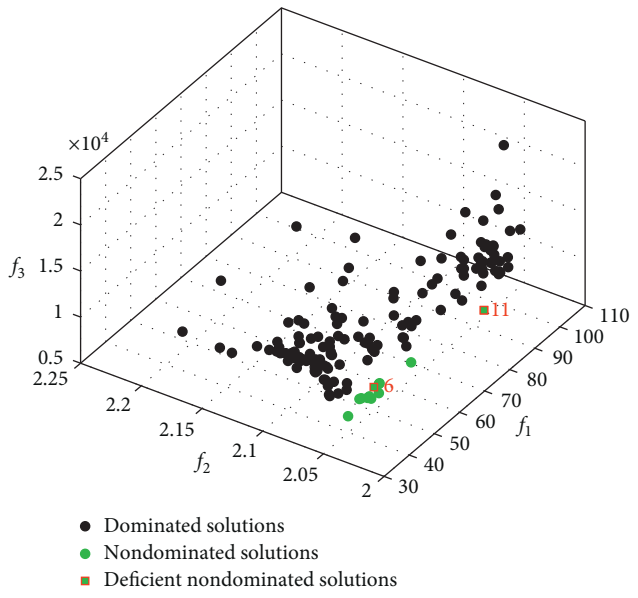

Figure 8: Distribution of multi-Pareto solutions.

Figure 10, the process of the FGI-PID controller is given as follows:

Step 1 (initialization): It is a process of setting the initial parameter, such as outputs $y(1)$ and $y(2)$, errors $e(1)$ and $e(2)e(1)$, control laws $u(1)$ and $u(2)$, and the six data are all equal 0 and will be updated in the process. Meanwhile, initializing the rate of reaction K_0, the stability effect η_0, k_i', k_d', the length of the production base sequence n, the weight coefficient w, and the fuzzy controller.

Step 2 (calculating the output and the error): It is a process of calculating the current output and acquiring current error. Generally, the first output of the system based on the initial data is 0.

Step 3 (calculating the correction coefficient β): There are two constraints for the calculation of β, including that whether the length of error sequence meet a certain number n, and whether the consecutive errors are all equal 0. If the length of error sequence less than n or errors $e(t-n+2)$ to $e(t)$ are all equal 0, w equals 1. when the length is more than n and these errors are not all equal 0, predictive error $e'(t+1)$ are acquired based on n errors and GM(1,1). In addition, if the current error $e(t)$ and $e'(t+1)$ are not both equal to zero, the correction coefficient β is calculated according to the deviation level between the current error and the predicted error. Formula (13) is aiming to calculate the correction coefficient β based on a logit function with a range of [0.5, 1] in the study, where the e of e^{β_0} is the Napierian base.

$$\beta_0 = \frac{\min\left(|e(t)|, |e'(t+1)|\right)^2}{\max\left(|e(t)|, |e'(t+1)|\right)^2}, \tag{12}$$

$$\beta = \frac{e^{\beta_0}}{1+e^{\beta_0}}. \tag{13}$$

Step 4 (adjusting the parameters K and η of the FGI-PID controller): K and η are calculated according to Formulas (14) and (15) by introducing a weight coefficient w to balance the original parameters and the modified parameters. The value of w can be determined by experience or test. For the FI-PID controller, parameters of K and η are fixed, w equals 1 all through.

$$K = K_0(w + (1-w)\beta), \tag{14}$$

$$\eta = \eta_0(w + (1-w)\beta). \tag{15}$$

Step 5 (calculating the control law and judging the task progress): Calculating the control law according to Formula (3). If the control task is completed, stop. Otherwise, update the data and return to Step 2.

The pseudocode corresponding to the simulation process of FGI-PID is shown as follows (Algorithm 3).

5. Test and Comparison of Controllers for ATO System

5.1. Test Method. To test the feasibility of the FI-PID controller and the FGI-PID controller, the train's dynamic model (Formula (2)) was taken as the control object, and a velocity-time curve from the Shanghai maglev demonstration line was used as the input signal to analyze and compare the performance of FI-PID and FGI-PID. The time interval of the original velocity-time curve is 1 s, and a curve with the interval of 0.1 s was acquired by interpolation with the method of "cubic" in MATLAB. MATLAB software is also the simulation environment in the study.

Table 2: Parameters and fitness of the new Pareto solutions.

No.	K	η	k_i'	k_d'	f_1	f_2	f_3
1[a]	196.056 906	0.004 112	2.483 254	11.076 463	33.840 311	2.037 480	8790.987 535
2	163.753 696	0.067 833	3.283 048	14.514 336	42.594 627	2.046 223	8207.051 904
3	163.753 696	0.067 833	3.353 620	14.514 336	47.685 838	2.048 811	7175.217 023
4	163.753 696	0.143 479	3.353 620	14.514 336	47.991 836	2.048 005	6891.833 427
5	163.753 696	0.157 608	3.283 048	14.514 336	46.123 175	2.046 986	7447.494 305
6[b]	163.990 325	0.049 013	3.450 764	14.514 336	52.744 138	2.055 492	6678.679 570
7	163.990 325	0.067 833	3.283 048	14.514 336	43.074 668	2.045 939	8191.242 857
8	163.990 325	0.067 833	3.283 048	14.831 223	61.992 764	2.043 818	7797.083 067
9	163.990 325	0.067 833	3.450 764	14.514 336	54.797 450	2.055 114	6669.372 779
10	163.990 325	0.157 608	3.353 620	14.514 336	51.153 823	2.047 966	6775.205 121
11[b]	192.644 021	0.169 557	9.476 489	28.630 928	82.011 092	2.025 346	9718.480 946
12	163.990 325	0.157 608	3.450 764	14.514 336	54.636 489	2.055 159	6623.210 587

[a]Individual in Table 1. [b]Individuals with the maximum fitness value.

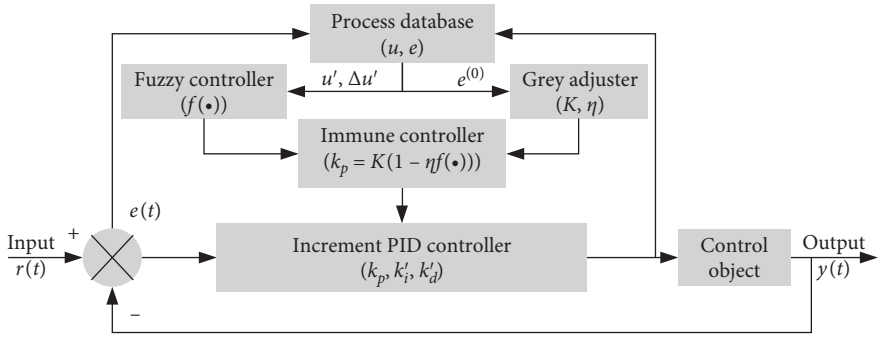

Figure 9: Structure of the FGI-PID controller.

The velocity-time curve and acceleration curve are shown in Figure 11. The planned driving distance is 29108.992 m, and the travel time is 441 s. The largest velocity is 431.28 km/h, the maximal acceleration is 0.950 m/s^2, the minimal deceleration is −0.931 m/s^2, and the maximal change rate of acceleration is 0.145 m/s^3.

During the simulation, the parameters of K, η, k_i', and k_d' were consistent with Table 2, excluding the 5th and 11th parameters. In terms of the grey predictive process, the modeling dimension n of GM(1,1) was set as 3; that is, when the prediction condition is satisfied, the next error $e\prime(t+1)$ would be predicted based on 3 consecutive errors. For the weight coefficient of the FGI-PID controller in the study, w was identified as 0.85 based on multiple tests, which were conducted between 0.5 and 0.95 by taking 0.05 as the step length.

5.2. Results. In an actual operation, ATO system receives operation commands from the ATP and ATS system continuously and performs commands such as traction, coasting, and braking to meet operation requirements. In the study, the simulations were used to analyze the applicability of the FI-PID controller and the FGI-PID controller for the ATO system. The applicability of the two controllers for ATO system had been analysed from the aspect of the traceability and comfort based on output results.

5.2.1. Traceability. The study analysed the traceability from the perspective of error. In general, the smaller the error, the better the traceability. The analysis process involved the objective functions (f_1, f_2, f_3) above and the maximal error. And minimum, maximum, average, and standard deviation of these error indicators were also computed.

As shown in Table 3, all of the FI-PID controllers and the FGI-PID controllers have shown good traceability. The maximum error value is 1.957, the maximum value of integrated absolute error (IAE) is 210.068, the maximum value of integral of time's reciprocal multiplied by squared error (ITRSE) is 0.062, and the maximum value of integral of time multiplied by squared error (ITSE) is 213 868.345. The length of the input sequence is 4421, and the results indicate that the above error is acceptable within a certain range.

Figure 12 shows the tracking curves with 1st parameters and 12th parameters in Table 3. Intuitively, it is almost impossible to see a major deviation, and both parameters show good traceability. Combined with Table 3, the 1st parameters show the best performance in the above indicators; that is, the corresponding error indicators are all minimum values for FI-PID and FGI-PID. For the 1st parameters, the IAE of the tracking process is 115.397 for FI-PID, and 112.779 for FGI-PID, the average error is 0.026 1 for FI-PID, and 0.025 5 for FGI-PID, and the maximal error is 1.871 for FI-PID, and 1.849 for FGI-PID. The ITRSE and

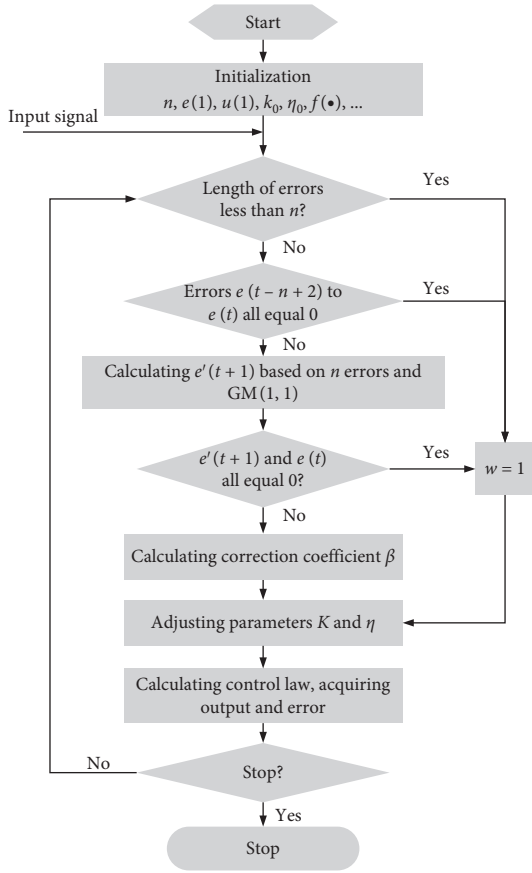

Figure 10: Process of the FGI-PID controller.

ITSE are 0.049 and 173 372.887 for FI-PID, and 0.048 and 166 347.702 for FGI-PID, respectively, which show a good performance in the initial stage and later stage. As a randomized control group, the results of the 12th group, similar to other parameters, are not as good as those of the 1st group. For the parameters, the average error is 0.047 5 for FI-PID, and 0.029 4 for FGI-PID, and the maximal error is 1.945 for FI-PID, and 1.923 for FGI-PID. Further, combined with Figure 13, it can be seen that the errors are mostly concentrated below 0.5. When the condition changed from traction to coasting, there is a short-term deviation of the tracking curves, which are slightly lower than the target curve, as shown in the partial diagrams in Figure 12 and the maximal errors in Table 3. These show that the results of NSGA-II based parameter tuning method in the study is suitable for both FI-PID and FGI-PID. Meanwhile, all of FI-PID and FGI-PID have good traceability with the same optimized parameters.

In terms of the comparison between the FI-PID controller and the FGI-PID controller, the values of indicators' minimum, maximum, average, and standard deviation of FGI-PID are all better than FI-PID in Table 3. Taking error sequence as an example, Figure 13 shows the sequence of the 1st parameters and the 12th parameters. For the 1st parameters, the error curves of FI-PID and FGI-PID are very close (Figure 13(a)), and there is no significant difference between them. This may be because the parameters are ideal, and there is less space for a further optimization. In addition, as can be seen from the results of Table 3, the maximum error and the objective function fitness values of FI-PID with 1st parameters are all larger than FGI-PID. Furthermore, according to Figure 13(b), it can be clearly seen that the error fluctuation of FI-PID is more severe than that of the FGI-PID controller, which results in a poor performance. Similar phenomenon can be seen from the results of other control parameters, as shown in Table 3 and Appendix. To an extent, FGI-PID can handle errors, especially for the overall errors.

Figure 14 shows the variation of the value of correction coefficient. It can be seen that the fluctuation of correction coefficients is very obvious. With the changes of the correction coefficient, the immune parameters (K and η) of the FGI-PID controller also change accordingly, and these changes had made the performances better. It is worth mentioning that the control effect of FGI-PID under different control parameters is relatively close, which can be seen from the smaller standard deviation in Table 3. In this regard, for FI-PID, the performance is not as good as FGI-PID, and the values of the standard deviation are greater.

Initialize the parameters (K_0, η_0, k_i', k_d', fuzzy rules $f(\cdot)$, control law u, initial output y, initial error e, length of the production base sequence n, and weight coefficient w).
while ($t \leq length\ of\ inputs$) **do**
  Calculate the current output $y(k)$ according to (1) or (2), and calculate current error $e(t)$
  if ($t \geq n$) and errors $e(t-n+2)$ to $e(t)$ are not all equal 0
    Calculate $e'(t+1)$ according to (8)–(11)
    if one of $e'(t+1)$ and $e(t)$ is not equal 0
      Calculate the correction coefficient according to formulas (12) and (13).
      Calculate K and η according to weight coefficient w, (14) and (15)
    else
      $K = K_0$, and $\eta = \eta_0$
    end if
  else
$K = K_0$, and $\eta = \eta_0$
  end if
$k_p(t) = K(1 - \eta f(u\prime(t), \Delta u\prime(t)))$
  Calculate the current control law $u(t)$ according to (3)
  Update data u, e, y
end while
Postprocess results and visualization

Algorithm 3

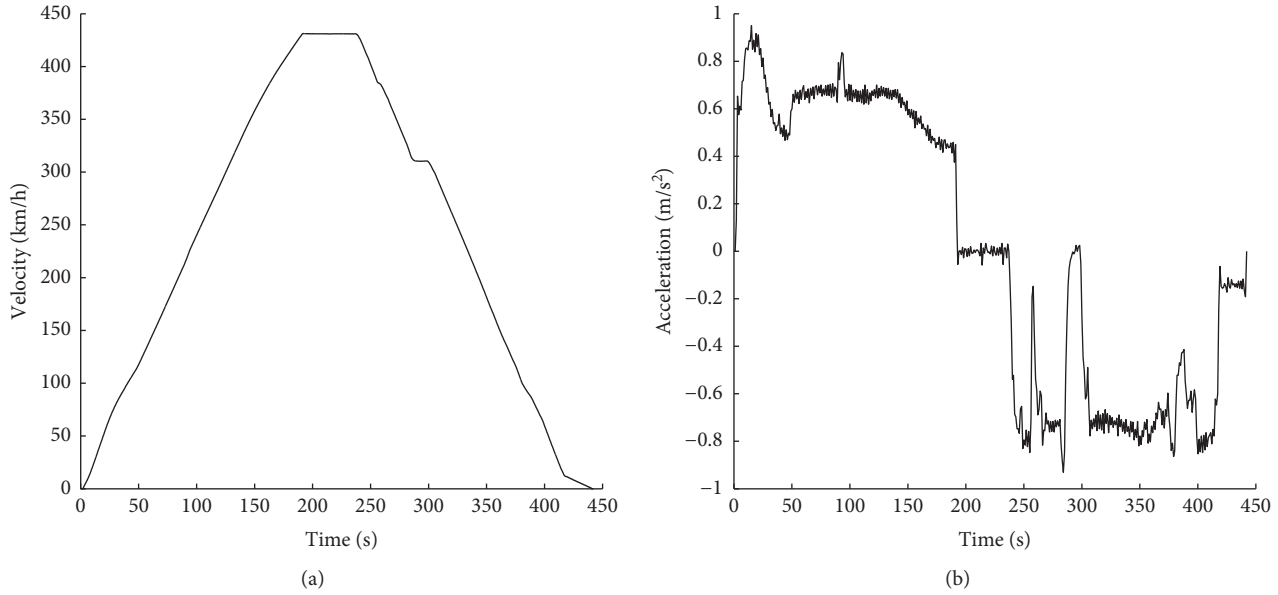

Figure 11: Velocity-time curve (a) and acceleration curve (b).

5.2.2. Comfort Level. The comfort level can be estimated from the point of accelerations. For example, in order to reduce the passenger's discomfort during a journey, the acceleration should be usually less than 1 m/s^2, and the change rate of acceleration (the derivative of acceleration) should be usually less than 0.75 m/s^3 [43, 59]. These common indicators were calculated in this study, as shown in Table 4.

Table 4 shows three acceleration indexes of velocity-time curves with the different controller and different parameter, including the maximum acceleration, the minimum deceleration, and the maximum change rate of acceleration, as well as their maximum, minimum, average, and standard deviation. Overall, the maximum acceleration under different parameters is 0.982 m/s^2, and the average value (0.950 485 m/s^2) is close to the target curve (0.950 m/s^2). The minimum deceleration is −0.942 m/s^2, and the average value (−0.931 487 m/s^2) is also close to the target curve (−0.931 m/s^2). The maximum acceleration change rate is 0.163 m/s^3, and the average value (0.161 185 m/s^3) is slightly larger than the target speed curve of 0.145 m/s^3. The accelerations and the change rates of

Table 3: Errors under different parameter and different controller.

No. [a]	f_1		f_2		f_3		Maximal error	
	FI-PID	FGI-PID	FI-PID	FGI-PID	FI-PID	FGI-PID	FI-PID	FGI-PID
1	115.397	112.779	0.049	0.048	173 372.887	166 347.702	1.871	1.849
2	190.398	126.056	0.057	0.052	200 737.828	183 424.269	1.924	1.896
3	193.596	124.591	0.059	0.052	204 386.149	181 710.911	1.937	1.891
4	197.444	130.052	0.056	0.055	190 142.383	192 790.746	1.888	1.925
5	206.014	134.077	0.061	0.056	211 369.137	197 974.489	1.951	1.937
7	189.967	126.185	0.059	0.052	205 235.797	183 856.682	1.942	1.898
8	203.835	132.220	0.061	0.055	210 307.087	192 813.168	1.945	1.922
9	192.035	120.538	0.059	0.051	203 369.217	179 641.669	1.937	1.887
10	207.309	131.984	0.062	0.055	213 868.345	195 433.065	1.957	1.933
12	210.068	130.027	0.061	0.054	211 001.222	192 005.118	1.945	1.923
Min	115.397	112.779	0.049	0.048	173 372.887	166 347.702	1.871	1.849
Max	210.068	134.077	0.062	0.056	213 868.345	197 974.489	1.957	1.937
Mean	190.606	126.851	0.058	0.053	202 379.005	186 599.782	1.930	1.906
S.D.	27.457	6.427	0.004	0.002	12 279.062	9 508.092	0.028	0.027

[a]Consistent with the original number in Table 2.

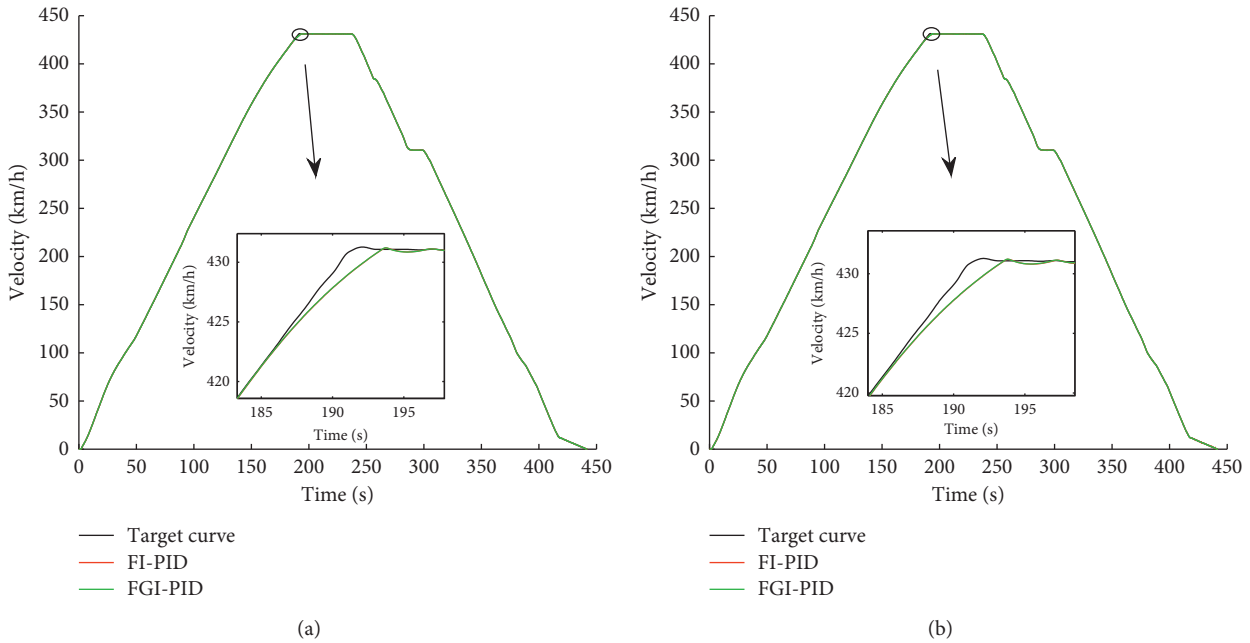

Figure 12: Tracking curves with 1st parameters (a) and 12th parameters (b).

acceleration satisfy the general requirements for comfort in urban rail transit.

When comparing the FI-PID controller and the FGI-PID controller with the performance of comfort level, the two are very close. The average value of acceleration and deceleration of FI-PID is slightly smaller than that of FGI-PID, but the stability is not as good as FGI-PID due to the larger standard deviations. At the same time, the maximum value of the acceleration change rate for FI-PID is not as good as FGI-PID, showing a larger value of the average and a larger value of the standard deviation. The performance on the value of the standard deviation in Table 4 is very close to Table 3 with a similar smaller standard deviation for FGI-PID.

In addition, Figures 15 and 16 show the changes in the acceleration and the change rate of acceleration with the 1st and 12th parameters. For the 1st parameters, the curves from different controllers are very close, which benefited from the suitability of the control parameters. But for the 12th parameters, the deviation of the two controllers' output can be found, which is more obvious fluctuation of FI-PID than that of FGI-PID. Combining Table 4 and Figure 14, FGI-PID can help reduce the fluctuation of acceleration and its change rate with a better traceability. It is worth mentioning that these phenomena are related to the variation of error. That is, the smaller the deviation on the velocity, the smaller the deviation on the acceleration.

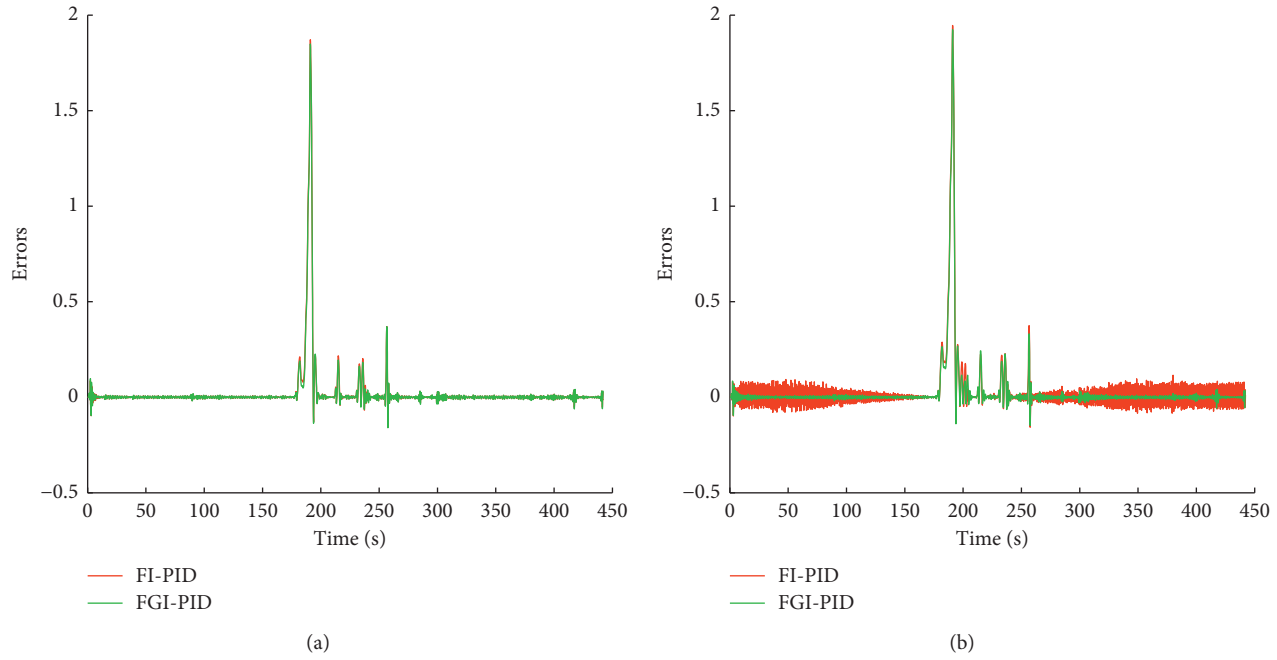

Figure 13: Error curves with 1st parameters (a) and 12th parameters (b).

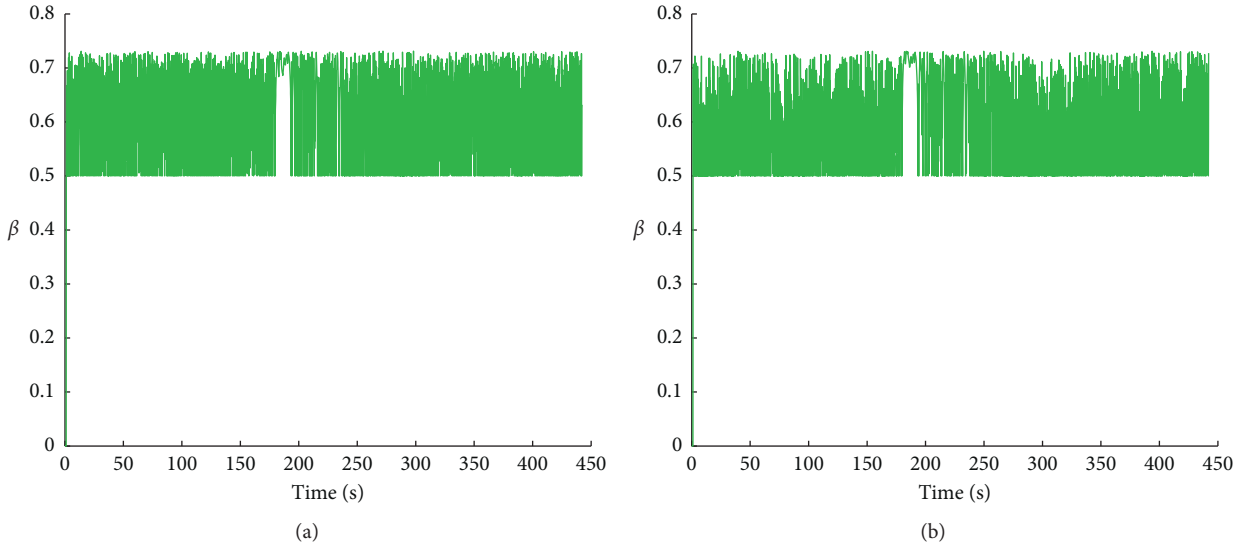

Figure 14: Changes of correction coefficient β with 1st parameters (a) and 12th parameters (b).

6. Discussion

Based on the parameter tuning and the development of the FI-PID controller, this paper studied the application of NSGA-II in parameter tuning and discussed the suitability of GM(1,1) integrated in the FI-PID controller. The test results show the feasibility of these methods.

In the case there are multiple optimization objects in a parameter tuning process, if they are merged into one optimization objective function, it is likely that the optimal result is not ideal because of different dimensions or magnitudes of objectives. And using multiobjective optimization algorithms is an ideal choice. Optimization algorithms are usually easy to get a feasible solution, but they are difficult to get a global optimal solution. This is also true for NSGA-II because the algorithm is random in generating individuals and genetic operations, and the selection of its parameters is also very important. The method of increasing the size of the population or running the optimal process multiple times is feasible for obtaining some better optimal

Table 4: Accelerations under different parameter and different controller.

No.[a]	Maximal acceleration (m/s^2)		Minimal deceleration (m/s^2)		Maximal change rate of acceleration (m/s^3)	
	FI-PID	FGI-PID	FI-PID	FGI-PID	FI-PID	FGI-PID
1	0.953 352	0.953 540	−0.932 446	−0.932 778	0.160 953	0.160 107
2	0.942 791	0.953 228	−0.941 354	−0.932 023	0.161 160	0.160 715
3	0.936 699	0.953 166	−0.932 546	−0.932 030	0.161 880	0.161 110
4	0.949 322	0.953 107	−0.930 687	−0.931 767	0.162 234	0.160 573
5	0.950 432	0.952 880	−0.941 854	−0.931 863	0.160 856	0.160 309
7	0.943 531	0.953 214	−0.942 312	−0.931 938	0.161 680	0.160 709
8	0.982 397	0.952 635	−0.929 668	−0.931 794	0.161 947	0.160 390
9	0.932 753	0.953 207	−0.918 563	−0.931 963	0.161 498	0.161 626
10	0.949 438	0.953 058	−0.910 764	−0.931 881	0.160 860	0.161 288
12	0.936 821	0.954 138	−0.929 015	−0.932 487	0.162 710	0.161 091
Min	0.932 753	0.952 635	−0.942 312	−0.932 778	0.160 856	0.160 107
Max	0.982 397	0.954 138	−0.910 764	−0.931 767	0.162 710	0.161 626
Mean	0.947 754	0.953 217	−0.930 921	−0.932 052	0.161 578	0.160 792
S.D.	0.013 957	0.000 401	0.010 151	0.000 325	0.000 629	0.000 478

[a]Consistent with the original number in Table 2.

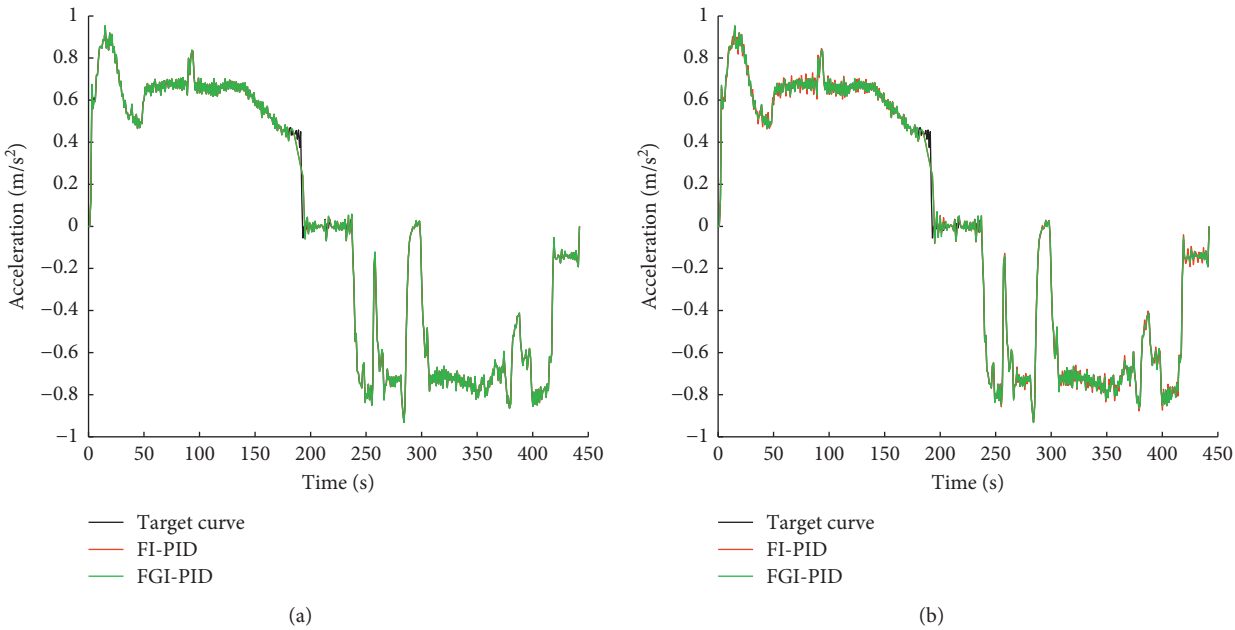

Figure 15: Acceleration curves with 1st parameters (a) and 12th parameters (b).

solutions. In this paper, based on 10 tuning processes, 148 solutions were further screened, 10 optimal individuals were finally determined, and the results also showed good performances. The process with a small population and iterations spends 948.128 s for the results in Table 1. It is also feasible to increase the size of the population, but the population with greater size or iterations will mean greater time consumption if, unfortunately, local optimal solutions are unsatisfactory situations. For practice, in order to acquire a better optimal solution or a better performance, it is usually worth the time to continually refine these key parameters.

The tests based on the velocity-time curve show that the FI-PID controller and the FGI-PID controller have good applicability, which can be attributed to FI-PID itself and has the property of the fuzzy control, and FGI-PID adds a prediction part to dynamically adjust immune parameters, which is similar to prediction control [20, 25, 37]. The difference of FGI-PID than FI-PID is that it can predict a next error based on historical errors and applies prediction error in the control process. In this study, based on the approximation idea of logit model, a logit function was used to generate and adjust the value of the correction coefficient based on the deviation between current errors and prediction errors. Meanwhile, to minimize possible adverse effects, the weighted average method was used to maintain the balance between initial parameters and modified

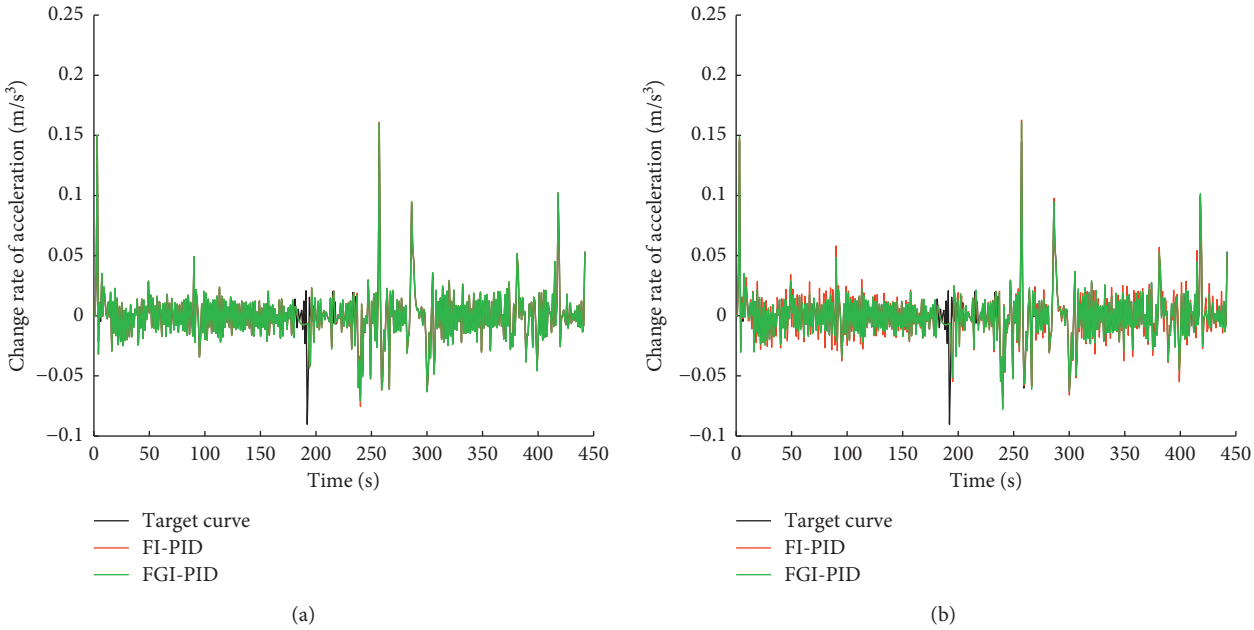

Figure 16: Change rate curves of acceleration with 1st parameters (a) and 12th parameters (b).

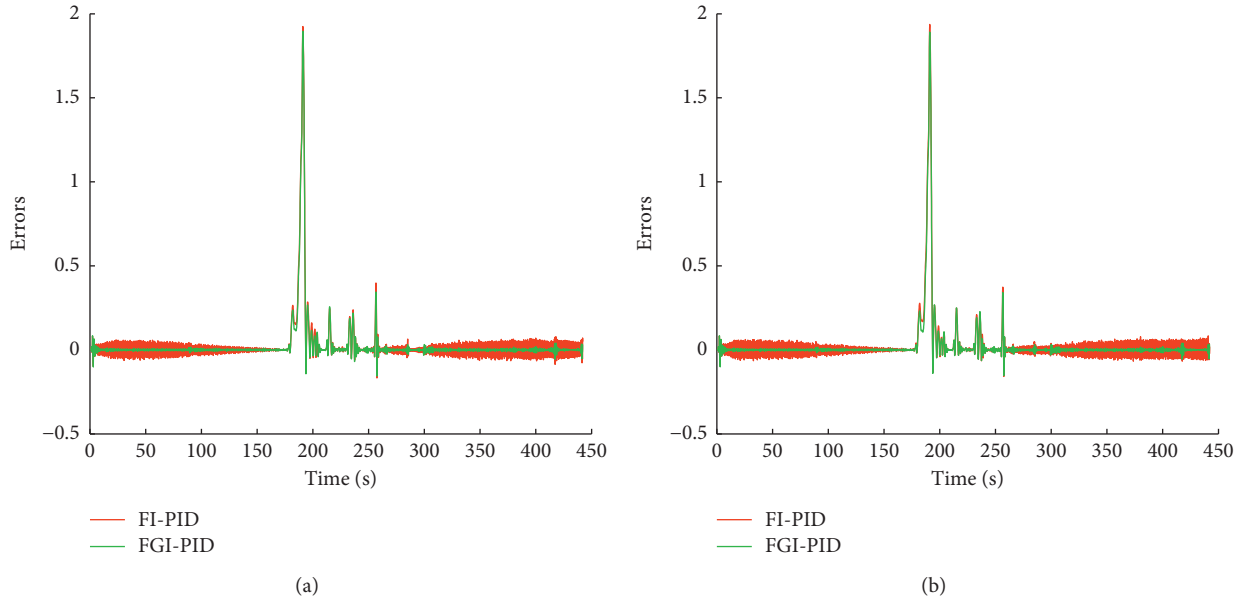

Figure 17: Error curves with 2nd parameters (a) and 3rd parameters (b).

parameters. The results show that the proposed method is feasible for the FI-PID controller, not only for better parameters but also for worse parameters. This is indicated by smaller standard deviations and averages, which mean that the outcomes of control effect are less uncertain and more likely to get a good performance. In this paper, the weight coefficient in the weighted average method and the length of the production base sequence in the prediction method are determined based on the manual testes, and there is a great space for optimizing these parameters. For practice, in order to acquire a better performance, these parameters can also be determined by optimization method or enumeration method with simulation analyses. In addition, the applicability of FI-PID and FGI-PID for other plants remains to be studied.

In an actual ATO system, the target velocity of a train is usually adjusted and issued by the corresponding ATP system during operation in real-time, rather than a fixed velocity profile generated before departing from a station. The test method in the study can only discuss controllers' performances from the aspects of traceability and comfort level limitedly. The research on train's punctuality or stopping accuracy for the controllers needs to add more simulation modules. However, the better the traceability is, the closer it is to the target curve and the smaller the running

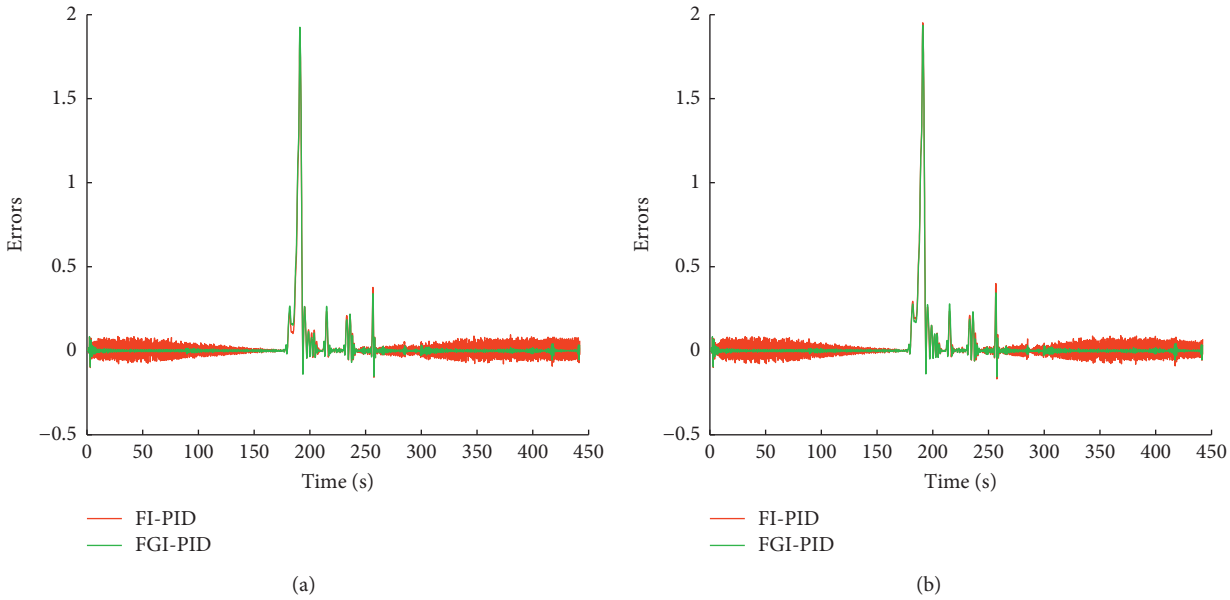

Figure 18: Error curves with 4th parameters (a) and 5th parameters (b).

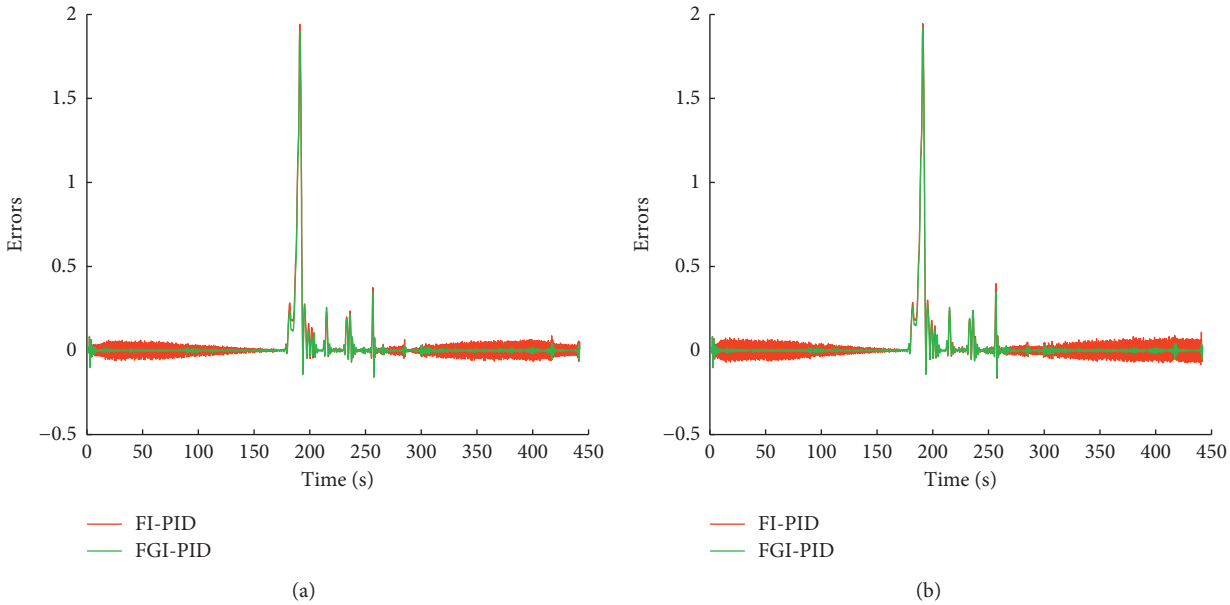

Figure 19: Error curves with 7th parameters (a) and 8th parameters (b).

deviation on the timing or the distance. Meanwhile, if a velocity curve was less adjusted during a control process, the workload of ATC system would also reduce more. An excellent controller can improve the stability of ATO systems.

7. Conclusion

In this paper, a parameter tuning framework for the FI-PID controller was constructed based on NSGA-II, a novel controller named FGI-PID was developed based on FI-PID and a method named GM(1,1), and the applicability of the FI-PID controller and the FGI-PID controller for an ATO system was analysed. The results showed that the parameter tuning method is feasible, with both FI-PID and FGI-PID have high applicability for the ATO system. At the same time, the performances of FGI-PID are better than FI-PID. For future studies, the parameter configuration of FGI-PID and the performance of the two controllers in a more complex and realistic simulation environment are worth discussing.

Appendix

Here, the error sequences corresponding to the 8 sets of optimized parameters in Table 2 are shown as Figures 17–20.

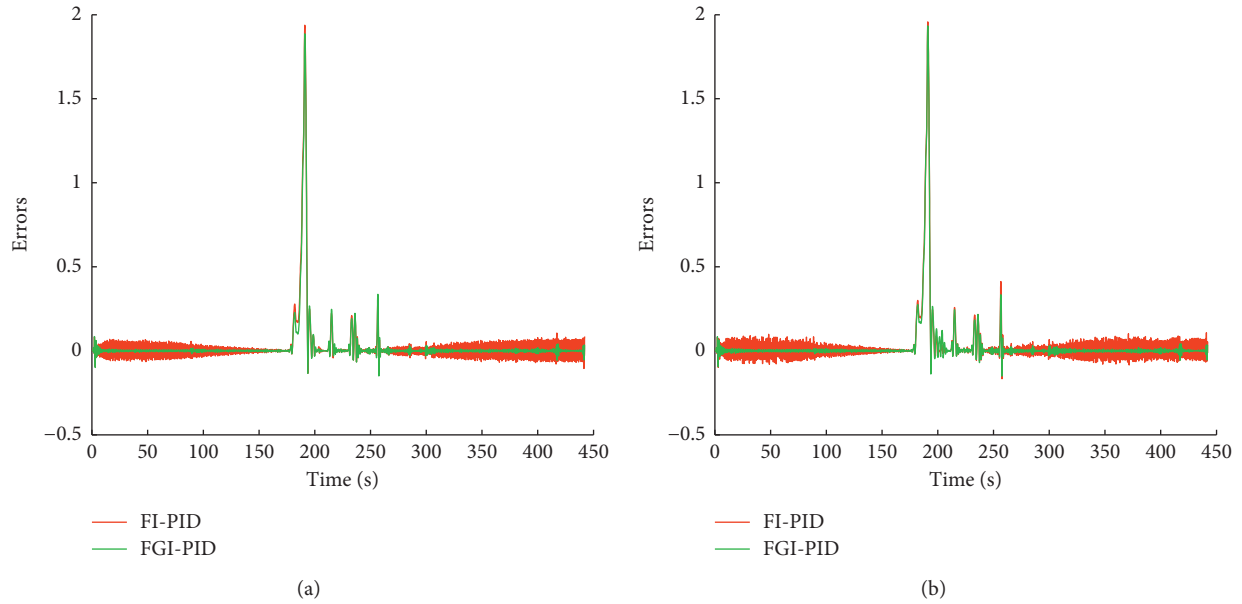

Figure 20: Error curves with 9th parameters (a) and 10th parameters (b).

These error curves can also show that the FGI-PID controller and the FI-PID controller have good performances. For more details, please refer to Tables 3 and 4.

Data Availability

The data used to support the findings of this study are available from the corresponding author upon request.

Conflicts of Interest

The authors declare no conflicts of interest.

Acknowledgments

This research was supported by the National Key R&D Program of China under grant 2016YFB1200602-02, the Science Research Project of Shanghai Science and Technology Committee under grant 18DZ1205803, and the International Exchange Program for Graduate Students, Tongji University, under grant 20190101. Specifically, the authors want to thank professor Jimin Zhang from Institute of Rail Transit, Tongji University, engineer Yijun Chen, Huahua Zhao, and Fangqi Zhang from Tongji University Maglev Transportation Engineering R&D Centre, and Ph.D. candidate Linjie Ren and Chen Chen from Key Laboratory of Road and Traffic Engineering, Ministry of Education, Tongji University, who had given many useful advices for the study.

References

[1] Y. Cao, Z.-C. Wang, F. Liu, P. Li, and G. Xie, "Bio-inspired speed curve optimization and sliding mode tracking control for subway trains," *IEEE Transactions on Vehicular Technology*, vol. 68, no. 7, pp. 6331–6342, 2019.

[2] K. Liu, X. Wang, and Z. Qu, "Research on multi-objective optimization and control algorithms for automatic train operation," *Energies*, vol. 12, no. 20, 22 pages, 2019.

[3] B.-R. Ke, C.-L. Lin, and C.-W. Lai, "Optimization of train-speed trajectory and control for mass rapid transit systems," *Control Engineering Practice*, vol. 19, no. 7, pp. 675–687, 2011.

[4] X. Chen, Y. Zhang, and H. Huang, "Train speed control algorithm based on PID controller and single-neuron PID controller," in *Proceedings of the 2nd WRI Global Congress on Intelligent Systems*, pp. 107–110, Wuhan, Hubei, China, December 2010.

[5] R. D. Utomo and E. D. Widianto, "Control system of train speed based on fuzzy logic controller," in *Proceedings of the 2nd International Conference on Information Technology, Computer, and Electrical Engineering*, pp. 256–261, Semarang, Indonesia, October 2015.

[6] J. Xue, Y. Wang, H. Li, X. Meng, and J. Xiao, "Advanced fireworks algorithm and its application research in PID parameters tuning," *Mathematical Problems in Engineering*, vol. 2016, Article ID 2534632, 9 pages, 2016.

[7] M. Mahdavian, S. Sudeng, and N. Wattanapongsakorn, "Multi-objective optimization and decision making for greenhouse climate control system considering user preference and data clustering," *Cluster Computing*, vol. 20, no. 1, pp. 835–853, 2017.

[8] A. Behroozsarand and S. Shafiei, "Control of TAME reactive distillation using non-dominated sorting genetic algorithm-II," *Journal of Loss Prevention in the Process Industries*, vol. 25, no. 1, pp. 192–201, 2012.

[9] Z. Chen, X. Yuan, B. Ji, P. Wang, and H. Tian, "Design of a fractional order PID controller for hydraulic turbine regulating system using chaotic non-dominated sorting genetic algorithm II," *Energy Conversion and Management*, vol. 84, pp. 390–404, 2014.

[10] M. T. Özdemir, D. Öztürk, Ī. Eke, V. Çelik, and K. Y. Lee, "Tuning of optimal classical and fractional order PID parameters for Automatic generation control based on the bacterial swarm optimization," *IFAC-PapersOnLine*, vol. 48, no. 30, pp. 501–506, 2015.

[11] S.-Z. Zhao, M. W. Iruthayarajan, S. Baskar, and P. N. Suganthan, "Multi-objective robust PID controller tuning using two lbests multi-objective particle swarm optimization," *Information Sciences*, vol. 181, no. 16, pp. 3323–3335, 2011.

[12] G. Reynoso-Meza, J. Sanchis, X. Blasco, and J. M. Herrero, "Multiobjective evolutionary algorithms for multivariable PI controller design," *Expert Systems with Applications*, vol. 39, no. 9, pp. 7895–7907, 2012.

[13] M. Rahmani, H. Komijani, A. Ghanbari, and M. M. Ettefagh, "Optimal novel super-twisting PID sliding mode control of a MEMS gyroscope based on multi-objective bat algorithm," *Microsystem Technologies*, vol. 24, no. 6, pp. 2835–2846, 2018.

[14] S. Wang, Y. Jiang, and H. Yang, "Chaos optimization strategy on fuzzy-immune-PID control of turbine regulating system," *Journal of System Simulation*, vol. 18, no. 6, pp. 1729–1732, 2006.

[15] Y. Ma and L. Gu, "Fuzzy immune PID Control of hydraulic system based PSO algorithm," *Telkomnika - Indonesian Journal of Electrical Engineering*, vol. 11, no. 2, pp. 890–895, 2013.

[16] L. Wang and B. Xiao, "PID controller parameters tuning based on pole assignment optimal prediction for power station boiler superheated steam temperature," *International Journal of Engineering and Technology*, vol. 8, no. 2, pp. 88–93, 2016.

[17] D. H. Kim, "Robust PID control using gain/phase margin and advanced immune algorithm," *Wseas Transactions on Systems*, vol. 3, no. 9, pp. 2841–2851, 2004.

[18] J. Mendes, L. Osório, and R. Araújo, "Self-tuning PID controllers in pursuit of plug and play capacity," *Control Engineering Practice*, vol. 69, pp. 73–84, 2017.

[19] R. Wai and J. Lee, "Adaptive fuzzy-neural-network control for maglev transportation system," *IEEE Transactions on Neural Networks*, vol. 19, no. 1, pp. 54–70, 2008.

[20] V. Majdabadi-Farahani, M. Hanif, I. Gholaminezhad, A. Jamali, and N. Nariman-Zadeh, "Multi-objective optimal design of online PID controllers using model predictive control based on the group method of data handling-type neural networks," *Connection Science*, vol. 26, no. 4, pp. 349–365, 2014.

[21] X. Wang and S. Bian, "PID parameters self-tuning based on genetic algorithm and neural network," *Journal of Jilin University (Science Edition)*, vol. 56, no. 4, pp. 953–958, 2018.

[22] H. Oshima, S. Yasunobu, and S. I. Sekino, "Automatic train operation system based on predictive fuzzy control," in *Proceedings of the International Workshop on Artificial Intelligence for Industrial Applications*, pp. 485–489, Castellón, Spain, June 1988.

[23] S. Yasunobu, S. Miyamoto, and H. Ihara, "Fuzzy control for automatic train operation system," in *Proceedings of the 4th IFAC/IFIP/IFORS Conference*, pp. 33–39, Baden-Baden, Germany, April 1983.

[24] S. Gao, H. Dong, B. Ning, Y. Chen, and X. Sun, "Adaptive fault-tolerant automatic train operation using RBF neural networks," *Neural Computing and Applications*, vol. 26, no. 1, pp. 141–149, 2015.

[25] X. Mo, T. Tang, C. Dong, Y. Yao, and X. Yao, "A realization and simulation of ATO speed control module-predictive fuzzy control algorithm,," in *Proceedings of the 2013 IEEE International Conference on Intelligent Rail Transportation*, pp. 263–267, Beijing, China, September 2013.

[26] L. Fu, "Research on the speed control of automatic train operation system based on the novel PSO-B-BP-PID controller," *Advanced Materials Research*, vol. 354-355, pp. 906–912, 2012.

[27] P. Wu, Q.-Y. Wang, and X.-Y. Feng, "Automatic train operation based on adaptive terminal sliding mode control," *International Journal of Automation and Computing*, vol. 12, no. 2, pp. 142–148, 2015.

[28] W. Shi, "Research on automatic train operation based on model-free adaptive control," *Journal of the China Railway Society*, vol. 38, no. 2, pp. 72–77, 2016.

[29] T. Hou, Y.-y. Guo, and H.-x. Niu, "Research on speed control of high-speed train based on multi-point model," *Archives of Transport*, vol. 50, no. 2, pp. 35–46, 2019.

[30] Z. Long, Y. Li, and X. Wang, "On maglev train automatic operation control system based on Auto-Disturbance-Rejection control algorithm," in *Proceedings of the 27th Chinese Control Conference*, pp. 681–685, Kunming, China, July 2008.

[31] G. Hou, Z. Zhao, X. Bai, and R. Huang, "Fuzzy immune PID control used in no-load grid-connection for doubly-fed wind power system," in *Proceeding of the 11th World Congress on Intelligent Control and Automation*, pp. 3134–3138, Shenyang, China, July 2015.

[32] A. Dai, X. Zhou, and X. Liu, "Design and simulation of a genetically optimized fuzzy immune PID controller for a novel grain dryer," *IEEE Access*, vol. 5, pp. 14981–14990, 2017.

[33] X.-y. Ren, F.-s. Du, H.-g. Huang, and S.-b. Zhang, "Application of improved fuzzy immune PID controller to bending control system," *Journal of Iron and Steel Research International*, vol. 18, no. 3, pp. 28–33, 2011.

[34] K. Zhang, D. Dong, and H. Pan, "Safety and reliability of speed detection and location systems for high-speed maglev trains," in *Proceedings of the 15th COTA International Conference of Transportation Professionals*, pp. 1810–1819, Beijing, China, July 2015.

[35] J. Huang, Z. Wu, J. Shi, Y. Gao, and D. Wang, "Influence of track irregularities in high-speed maglev transportation systems," *Smart Structures and Systems*, vol. 21, no. 5, pp. 571–582, 2018.

[36] Y. Zhang, L. Zhang, and Z. Dong, "An MEA-tuning method for design of the PID controller," *Mathematical Problems in Engineering*, vol. 2019, Article ID 1378783, 11 pages, 2019.

[37] L. Hao, X. Wei, Z. Wang, and S. Zhou, "The study on self-adaptive predictive arithmetic based on RBF neural network applied in the proportion control of hydrogen and nitrogen in synthesis ammonia production,," in *Proceedings of the 2nd International Conference on Mechanic Automation and Control Engineering*, pp. 811–814, Inner Mongolia, China, July 2011.

[38] A. Li and M. Zhao, "Arithmetic predictive control on neural network," *Computer Engineering and Design*, vol. 28, no. 24, pp. 5931–5934, 2007.

[39] S. Liu and J. Deng, "The range suitable for GM(1,1)," *Systems Engineering-Theory & Practice*, vol. 20, no. 5, pp. 121–124, 2000.

[40] Y. Wang, Y. Dang, Y. Li, and S. Liu, "An approach to increase prediction precision of GM(1,1) model based on optimization of the initial condition," *Expert Systems with Applications*, vol. 37, no. 8, pp. 5640–5644, 2010.

[41] S. Oh, Y. Yoon, and Y. Kim, "Automatic train protection simulation for radio-based train control system," in *Proceedings of International Conference on Information Science and Applications*, pp. 1–4, Visakhapatnam, India, 2012.

[42] J. Farooq and J. Soler, "Radio communication for communications-based train control (CBTC): a tutorial and survey,"

IEEE Communications Surveys & Tutorials, vol. 19, no. 4, pp. 1377–1402, 2017.

[43] D. Li, J. Meng, S. Hao, and Z. Liu, "An intelligent train operation based on fuzzy adaptive PID," *Journal of Lanzhou Jiaotong University*, vol. 37, no. 4, pp. 27–33, 2018.

[44] Z. Yu and D. Chen, "Modelling and system identification of the braking system of urban rail vehicles," *Journal of the China Railway Society*, vol. 33, no. 10, pp. 37–40, 2011.

[45] W. Xu and B. Xiao, "Train control simulation based on CMAC-PID algorithm," in *Proceedings of 25th Chinese Control and Decision Conference*, pp. 4476–4480, Guiyang, China, May 2013.

[46] J. Meng and Z. Liu, "Research on intelligent algorithm for precise parking of urban rail transit based on predictive fuzzy PID," *Computer Engineering and Applications*, vol. 55, no. 23, pp. 257–264, 2019.

[47] X. Wang, R. Chen, and Z. Cai, "Simulation research on ATO System based on PID algorithm," *Railway Computer Application*, vol. 24, no. 4, pp. 44–47, 2015.

[48] H. Qi and W. Xu, "Design of maglev automatic train operation system and research on predictive control algorithm," in *Proceedings of the 2011 IEEE International Conference on Computer Science and Automation Engineering*, pp. 463–470, Shanghai, China, June 2011.

[49] H. Wang, "Research on speed control and automatic train operation system of maglev train (Ci xuan fu lie che su du kong zhi yu zi dong jia shi xi tong yan jiu)," *National University of Defense Technology*, Changsha, China, in Chinese, 2002.

[50] C. C. Alcala, S. Lin, R. He, and C. Briso-Rodriguez, "Design and test of a high QoS radio network for CBTC systems in subway tunnels,," in *Proceeding of the 2011 IEEE 73rd Vehicular Technology Conference*, pp. 1–5, Budapest, Hungary, May 2011.

[51] X. Liu, X. Chen, X. Zheng, S. Li, and Z. Wang, "Development of a GA-Fuzzy-Immune PID controller with incomplete derivation for robot dexterous hand," *The Scientific World Journal*, vol. 2014, Article ID 564137, 10 pages, 2014.

[52] S. Wang, Y. Jiang, and H. Yang, "Chaos optimization strategy on fuzzy-immune- PID control of the turbine governing system," in *Proceeding of the 2006 IEEE/RSJ International Conference on Intelligent Robots and Systems*, pp. 1594–1598, Beijing, China, November 2006.

[53] G. K. M. Pedersen and Z. Yang, "Multi-objective PID-controller tuning for a magnetic levitation system using NSGA-II," in *Proceedings of the 8th Annual Conference on Genetic and Evolutionary Computation*, pp. 1737–1744, Seattle, USA, July 2006.

[54] A. Harrag and S. Messalti, "Variable step size modified P&O MPPT algorithm using GA-based hybrid offline/online PID controller," *Renewable and Sustainable Energy Reviews*, vol. 49, pp. 1247–1260, 2015.

[55] K. Deb, A. Pratap, S. Agarwal, and T. Meyarivan, "A fast and elitist multiobjective genetic algorithm: NSGA-II," *IEEE Transactions on Evolutionary Computation*, vol. 6, no. 2, pp. 182–197, 2002.

[56] H. Hu, L. Xu, E. D. Goodman, and S. Zeng, "NSGA-II-based nonlinear PID controller tuning of greenhouse climate for reducing costs and improving performances," *Neural Computing & Applications*, vol. 24, no. 3-4, pp. 927–936, 2014.

[57] V. Babaveisi, M. M. Paydar, and A. S. Safaei, "Optimizing a multi-product closed-loop supply chain using NSGA-II, MOSA, and MOPSO meta-heuristic algorithms," *Journal of Industrial Engineering International*, vol. 14, no. 2, pp. 305–326, 2018.

[58] M. Cheng and G. Shi, "Improved methods for parameter estimation of gray model GM(1,1) based on new background value optimization and model application," *Communication in Statistics-Simulation and Computation*, vol. 201923 pages, 2019.

[59] Y. Zhang, Z. Chen, J. Wang, and P. Wu, "Research on the comfort control technology of the ATO system in high-speed railway," *Journal of Railway Engineering Society*, vol. 36, no. 3, pp. 67–71, 2019.